



# Prioritizing forestation based on biogeochemical and local biogeophysical impacts

Michael G. Windisch<sup>1,2,3</sup>✉, Edouard L. Davin<sup>1,4</sup>✉ and Sonia I. Seneviratne<sup>1</sup>

**Reforestation and afforestation is expected to achieve a quarter of all emission reduction pledged under the Paris Agreement. Trees store carbon in biomass and soil but also alter the surface energy balance, warming or cooling the local climate. Mitigation scenarios and policies often neglect these biogeophysical (BGP) effects. Here we combine observational BGP datasets with carbon uptake or emission data to assess the end-of-century mitigation potential of forestation. Forestation and conservation of tropical forests achieve the highest climate benefit at 732.12 tCO<sub>2</sub>e ha<sup>-1</sup>. Higher-latitude forests warm the local winter climate, affecting 73.7% of temperate forests. Almost a third (29.8%) of forests above 56° N induce net winter warming if only their biomass is considered. Including soil carbon reduces the net warming area to 6.8% but comes with high uncertainty (2.9–42.0%). Our findings emphasize the necessity to conserve and re-establish tropical forests and consider BGP effects in policy scenarios.**

Limiting global warming to +2°C or even +1.5°C above pre-industrial levels will require the removal of CO<sub>2</sub> from the atmosphere in addition to reducing CO<sub>2</sub> emissions to near-zero levels<sup>1</sup>. Land stewardship will play a crucial role in this endeavour, as recognized by the global scientific community in the special reports of IPCC on climate change and land<sup>2</sup> and on global warming of 1.5°C (ref. <sup>1</sup>), as well as by 187 countries in their nationally determined contributions (NDCs), the main guiding framework to reach the targets of the Paris Agreement<sup>3</sup>. A range of studies has since estimated the land sector's capability, and especially regards forests, to take up carbon<sup>4–6</sup>.

All these efforts rely on a profound change in land management. Most of the mitigation scenarios in line with limiting global warming to +2°C or below depend on land-based mitigation measures (bioenergy with carbon capture and storage (BECCS) and reforestation/afforestation) to capture 200–400 GtCO<sub>2</sub> within this century<sup>1,2</sup>. Forestation (defined here to include both reforestation and afforestation) is recognized as the most cost-effective and land-intensive land-based CO<sub>2</sub> removal option assessed in the IPCC special reports<sup>1,2</sup>. The proposed large-scale land-cover transitions under current emission reduction goals of parties under the Paris Agreement will influence climate by taking up carbon from the atmosphere, a biogeochemical (BGC) effect, but will also exert a biogeophysical (BGP) influence by changing environmental variables such as surface albedo and land evapotranspiration<sup>7</sup>. The latter effect is mostly neglected by mitigation policy and is also absent in scenarios produced by integrated assessment models, despite studies exploring the combined BGP and BGC effects for more than two decades<sup>8–10</sup>.

Depending on the type of land cover that is reforested or afforested, the regional background climate and the season, the cooling associated with the forest's carbon uptake is enhanced or counteracted by BGP effects. The lowered albedo of reforested and afforested areas acts against the cooling BGC impact. This effect is most pronounced in frequently snow-covered regions and can even lead to a net warming effect of forests in these conditions. Where newly established forests strengthen the evaporative capacity of the land, they cool the local environment by shifting the surface energy

balance from sensible to latent heat. Especially at lower latitudes, this effect supersedes the warming of the lowered albedo, resulting in a net cooling of the local environment in addition to the carbon uptake, thus, enhancing the benefit of establishing and conserving forests<sup>7,11</sup>.

Past studies compared the radiative forcing of BGP and BGC effects by assessing Earth System Model (ESM) experiments of global scale forestation or deforestation<sup>8,9,12–15</sup>. Here, we assess the importance of local BGP effects using two observation-based datasets of the local temperature response to land-cover transition produced by Bright et al. in 2017<sup>16</sup> and Duveiller et al. in 2018<sup>17</sup>. Instead of relying on the radiative forcing concept, which does not account for non-radiative processes such as changes in evapotranspiration and surface roughness<sup>18</sup>, we translate the temperature-based BGP effect into a CO<sub>2</sub>e (equivalent) metric. This metric uses the transient climate response to cumulative emissions (TCRE; ref. <sup>19</sup>) derived from Coupled Model Intercomparison Project Phase 5 (CMIP5) ESMs to convert from temperature to CO<sub>2</sub> emissions (Methods).

The BGC effect is determined by (1) the differences in above- and below-ground biomass carbon density between non-forest and forested vegetation of the IPCC Tier-1 biomass carbon density data<sup>20</sup> and (2) the soil organic carbon (SOC) response of the top 30 cm of soil to land-cover changes from or to forest<sup>21</sup> (Methods).

We note that our BGP CO<sub>2</sub>e metric only encompasses local temperature changes, ignoring other local and non-local carbon effects: for instance, reduced impacts in several other parts of the world, such as associated with reduced sea-level rise or attenuated increase in some extreme events<sup>1</sup>. Given the constraint from remote sensing data, we do not quantify potential BGP effects that depend on the size of the land-use change, such as changes in precipitation patterns of large-scale forestation or deforestation<sup>22,23</sup>. For each increment of forest area gained or removed, the BGC effect progressively changes its impact on the global climate system while the CO<sub>2</sub>e of the BGP effect measured per ha incrementally shapes the areal extent affected by BGP effects. The CO<sub>2</sub>e metric proposed here is, thus, a tool to compare and prioritize single forest sites and their climate impact. BGP effects that emerge from the scale of a

<sup>1</sup>Institute for Atmospheric and Climate Science, ETH Zurich, Zurich, Switzerland. <sup>2</sup>Potsdam Institute for Climate Impact Research, Potsdam, Germany.

<sup>3</sup>Humboldt-Universität zu Berlin, Berlin, Germany. <sup>4</sup>Present address: Wyss Academy for Nature, Climate and Environmental Physics, Oeschger Centre for Climate Change Research, University of Bern, Bern, Switzerland. ✉e-mail: [michael.gregory.windisch@alumni.ethz.ch](mailto:michael.gregory.windisch@alumni.ethz.ch); [edouard.davin@wyssacademy.org](mailto:edouard.davin@wyssacademy.org)

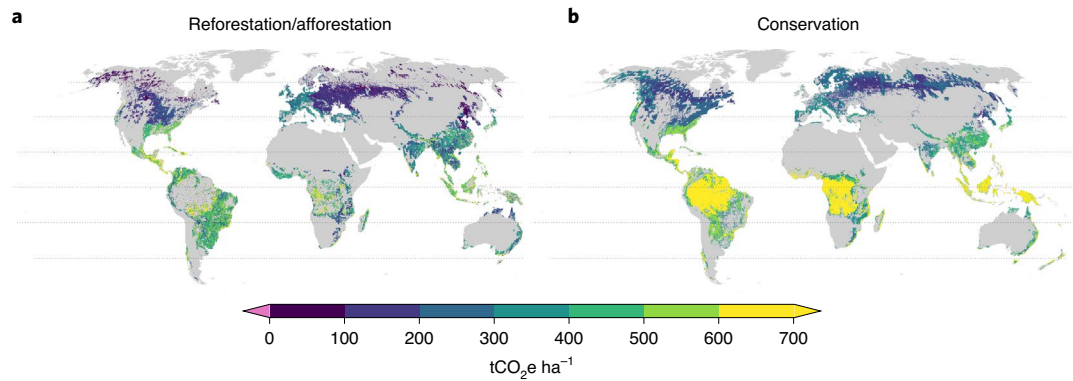


**Fig. 1 | Combined BGP and BGC mitigation potential of forestation and forest conservation. a, b**, The  $\text{CO}_2\text{e}$  of forestation (reforestation and afforestation) of current grassland, shrubland and cropland (**a**) and of avoided deforestation of standing forests (**b**) measured by the sum of their  $\text{CO}_2$  uptake (or avoided loss) in biomass and soil and the  $\text{CO}_2\text{e}$  of the local BGP effect induced. Base map adapted from GSHHG<sup>32</sup> and GMT<sup>33</sup>.

proposed forestation effort are not considered in the BGP datasets and cannot be encompassed by the  $\text{CO}_2\text{e}$  metric.

We report the combined BGC and local BGP effect of forestation and forest conservation sites by hectare. Non-forested sites (grassland, shrubland and cropland) determined by the GLC2000 land-cover map are assessed by their ability to take up additional carbon in their biomass and soil stores together with the local BGP impacts of transitions to a neighbouring forest within a  $0.25^\circ \times 0.25^\circ$  window. Already forested sites are evaluated by their avoided carbon release if they stay conserved in addition to the local BGP influence of their averted transition to the ‘cultivated and managed land’ land-cover type of the GLC2000 dataset.

In line with the most common time frame of emission pathways and climate trajectories, we consider the mitigation potential of forestation or forest conservation at the end of the century<sup>1</sup>. The processes encompassed by our study come into effect on different time scales. Newly established forests gradually take up  $\text{CO}_2$  from the atmosphere during their growth over many decades, while the albedo and evaporative transition might be in effect after a single decade<sup>24</sup>. The  $\text{CO}_2\text{e}$  effect assessed here represents the cumulative flux of the BGC carbon uptake and the BGP  $\text{CO}_2\text{e}$  effect over 80 yr. Processes within the 80-yr time frame, such as yearly variations or the difference between nearly instantaneous deforestation and gradual forest establishment, get aggregated in time. In this, we disregard their shape or form between now and the end of the century. This approach limits the applicability of our metric in more short-term goals that lie within our aggregated time horizon, such as prohibiting a  $1.5^\circ\text{C}$  overshoot scenario. We assume that conserved forests retain carbon in their biomass and keep albedo and evapotranspiration unchanged as long as they stay protected, neglecting potential processes in mature forests like carbon loss from diseases and windfall. Further, assume that the observed BGP and BGC effects are fully established after 80 yr in the case of forestation and forest conservation, which is in line with previous studies<sup>8</sup>.

Low latitudes that sustain tropical rainforests exceed all other regions in terms of climate benefit measured by the sum of the BGC and BGP  $\text{CO}_2\text{e}$  of forestation and forest conservation. Tropical forests achieve a mean mitigation potential of  $732.12 \text{ tCO}_2\text{e ha}^{-1}$  of removed or avoided emission (standard deviation  $\sigma = 167.45 \text{ tCO}_2\text{e ha}^{-1}$ ) (Fig. 1). The climate benefit of the same area of tropical forest is on average  $3.6\times$  ( $\sigma = 1.4$ ) and  $3.7\times$  ( $\sigma = 2.8$ ) higher than the one of temperate and boreal forests. Taking BGP effects into account constitutes  $+51.10 \pm 21.41 \text{ tCO}_2\text{e ha}^{-1}$  of the mitigation benefit of tropical regions and  $+31.80 \pm 24.32 \text{ tCO}_2\text{e ha}^{-1}$  of oceanic temperate forests by cooling the annual local temperature. In comparison, the benefit of BGP effects is markedly lower in temperate continental

( $12.02 \pm 17.90 \text{ tCO}_2\text{e ha}^{-1}$ ) and boreal ( $2.98 \pm 14.31 \text{ tCO}_2\text{e ha}^{-1}$ ) forests. Planting forests in the last two regions runs the risk of warming the local climate by BGP effects. This annual local warming response opposes the cooling influence of the carbon uptake at 22.7 and 38.8% of the total area of continental temperate and boreal regions. The warming BGP effect is even more pronounced in boreal winter, where 73.7 and 68.2% of the continental temperate and boreal area experience a reduction of their mitigation potential when considering BGP effects (Fig. 2).

Whether the BGP effect warms or cools the local climate is related to the latitude. North of  $56^\circ\text{N}$ , the median BGP response warms the annual local climate opposing the cooling influence of the BGC effect. During the boreal winter, this latitude threshold of detrimental BGP influence is pushed southward down to  $39^\circ\text{N}$  (red highlights, Fig. 2). Overall, 18.7% of forestation sites between  $39^\circ\text{N}$  and  $56^\circ\text{N}$  and almost a third (29.8%) above  $56^\circ\text{N}$  exert a net warming effect in boreal winter if only the above- and below-ground biomass is considered. Adding SOC to the mitigation benefit diminishes the areas with a net warming effect in boreal winter to 3.2% between  $39^\circ\text{N}$  and  $56^\circ\text{N}$  and 6.8% above. However, the uncertainty of the mitigation potential of the soil carbon uptake is considerable. If, instead of the median value between the different datasets estimating the BGP and BGC effects, a higher BGP and lower BGC estimate is used (median  $\pm \sigma$  for BGP/BGC), we find a wide range of area that exerts a net warming effect in winter when considering SOC (1.8–28.2% between  $39^\circ\text{N}$  and  $56^\circ\text{N}$  and 2.9–42.0% above  $56^\circ\text{N}$ ). In contrast, no local warming is induced by forests even at high latitudes during the boreal summer (Fig. 3). Regions where the BGP and BGC effects work in synergy and both a pronounced BGP cooling (higher than the global mean BGP plus standard deviation) and a high BGC effect (higher than the global mean BGC plus standard deviation) occur at the same site are located between  $23^\circ\text{N}$  and  $29^\circ\text{S}$  (yellow highlights, Fig. 2).

The high mitigation potential of low-latitude tropical forests on climate is predominantly produced by the vast amount of  $\text{CO}_2$  they store in their biomass. The  $\text{CO}_2\text{e}$  of the annually averaged BGP effects ranges between 4.7 and 18.3% (5th and 95th percentile) with a median of 6.4% compared to their BGC effect (Fig. 3). In temperate ( $-7.8$ – $38.9\%$ , median 6.4%) and boreal ( $-9.0$ – $15.4\%$ , median 1.4%) regions, the BGP effect experiences a higher variance and locally also opposes the cooling effect of the BGC effect. In the last two regions, the induced temperature change of BGP effects varies markedly with the seasons. In boreal summer, all temperate (8.7–57.2%; median 19.8%) and boreal (4.0–41.9%; median 18.0%) regions experience a BGP-induced local cooling of forests. This cooling influence during summer is reversed in winter

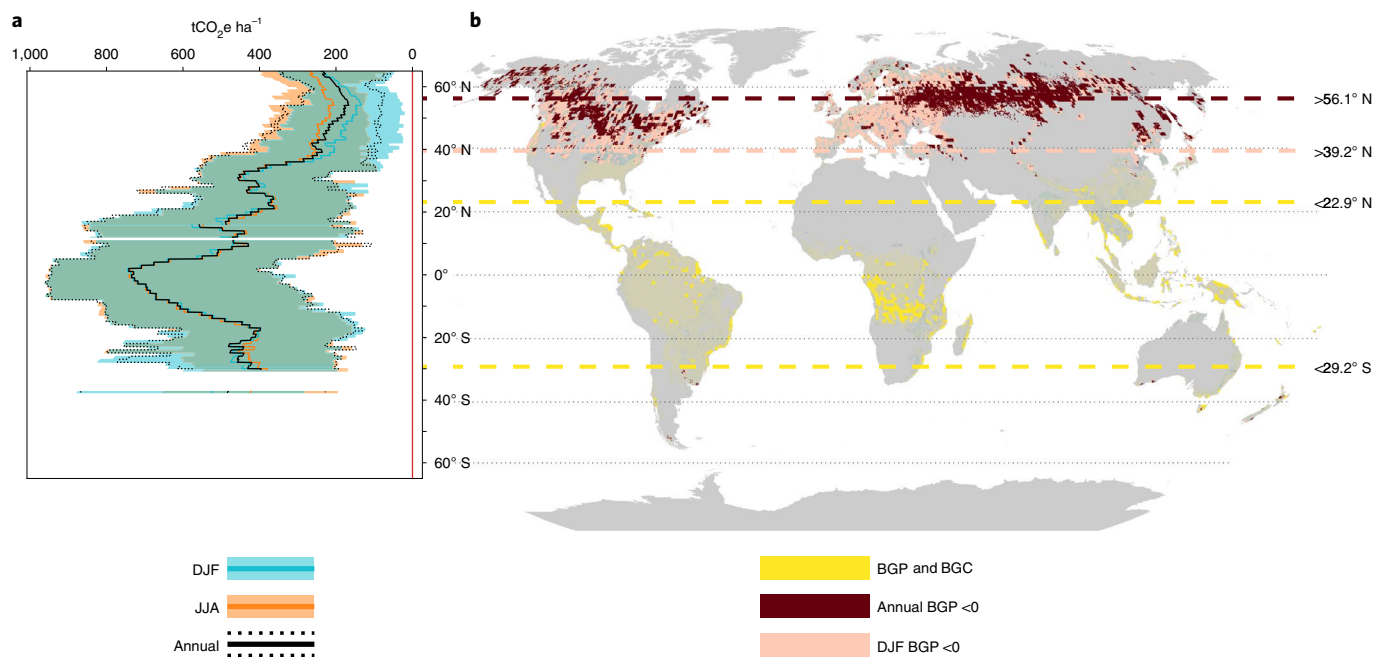


**Fig. 2 | Latitudinal dependence of the climate impact of forestation and forest conservation.** **a**, The 1° latitudinal averages of the sum of the BGC and local BGP impact of forestation and forest conservation with 10th and 90th percentile envelope. Only latitudes with >1.5% of the total grid cells covered by forest are considered. Depicted are the annual response (black) and the seasonal response in the boreal winter (DJF, December to February, blue) and summer (JJA, June to August, orange). **b**, Synergy and opposing effects between the BGP and BGC effects are highlighted. Sites in which the BGP influence opposes the response to BGC annually/in boreal winter are coloured in dark/light red. Areas of synergy between both effects (exceeding the mean plus standard deviation in both simultaneously) are shown in yellow. Emphasized by dashed lines are the lowest northern latitudes at which the latitudinal median BGP effect opposes the carbon uptake annually (56.1° N, dark red) and during boreal winter (39.2° N, light red). Further, the latitudinal bounds that envelope 98% of all synergistic areas (<22.9° N, >29.2° S) are shown by the dashed yellow lines. Base map adapted from GSHHG<sup>32</sup> and GMT<sup>33</sup>.

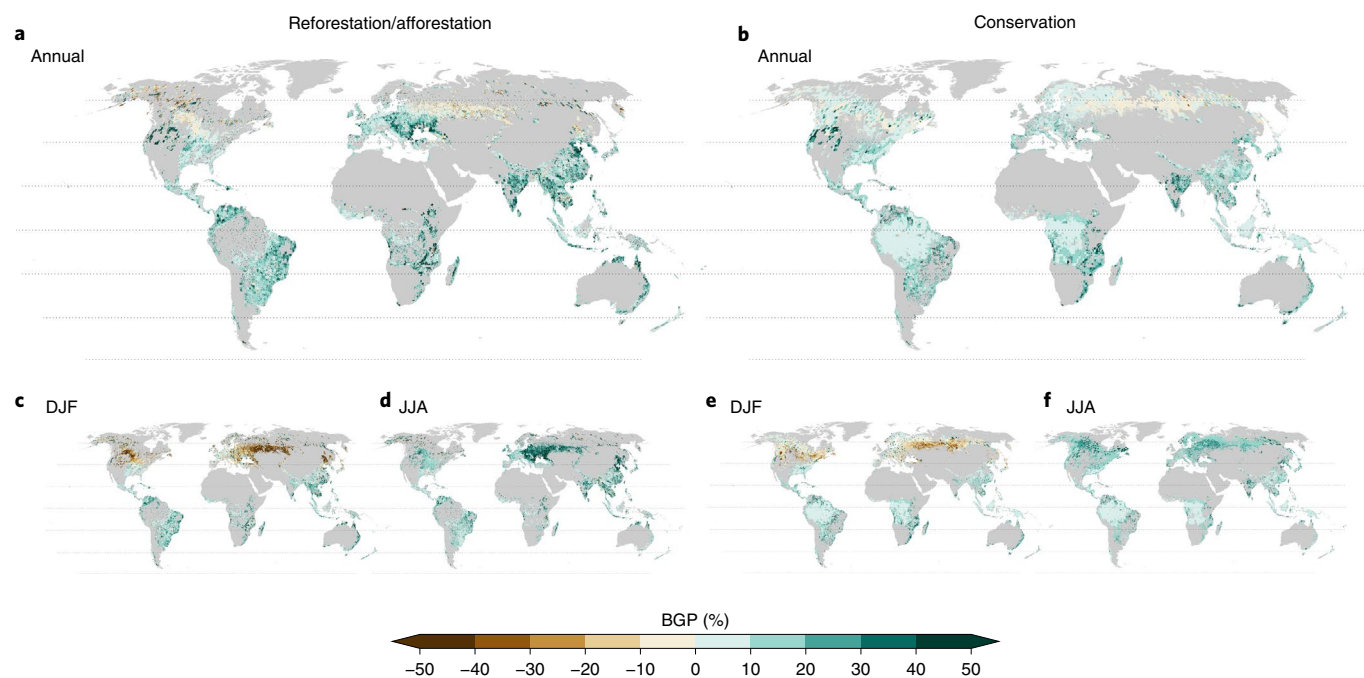


**Fig. 3 | Seasonality of the BGP impact of forestation and forest conservation.** Fraction of the BGP impact of forestation (reforestation and afforestation) and avoided deforestation on local climate expressed as CO<sub>2</sub>e compared to the effect of their CO<sub>2</sub> uptake or avoided loss in percentage. **a–f**, Fractions are reported for the annual average response of forestation (**a**) and conservation (**b**), the boreal winter response to forestation (**c**) and conservation (**e**), as well as the boreal summer response to forestation (**d**) and conservation (**f**). The impact of forestation is shown on the left; the one of conserved, standing forest on the right. Brown colours depict areas where BGP effects oppose the BGC impact, turquoise colours are assigned to areas where the cooling effect of the carbon uptake is locally enhanced by BGP processes. Base map adapted from GSHHG<sup>32</sup> and GMT<sup>33</sup>.

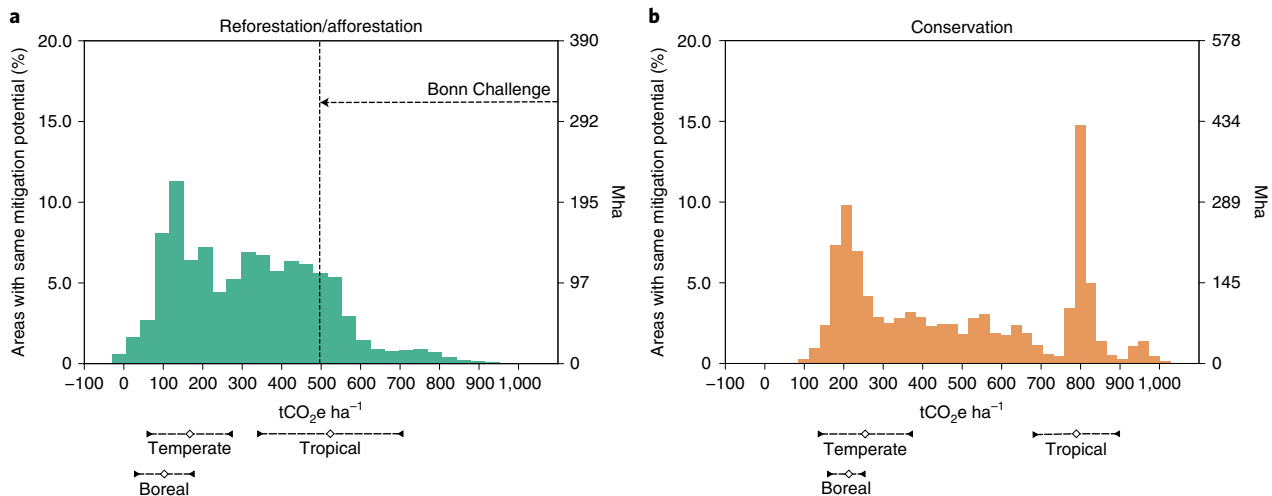


**Fig. 4 | Dominance of standing forests in areas of high mitigation potential.** **a, b**, Frequency of areas with the same mitigation potential (sum of BGC and local BGP effect) of reforestation and afforestation (**a**, green) and standing forest sites (**b**, orange) as percentages. The corresponding total area in Mha is depicted on the right y axis. The area envisioned in the Bonn Challenge (350 Mha) is added to the reforestation and afforestation distribution. Assuming that the reforestation and afforestation effort of the Bonn Challenge would start with the sites that hold the highest mitigation potential, that is, the strongest cooling (starting from the right), it would need to afforest all areas down to  $495.2 \text{ tCO}_2\text{e ha}^{-1}$  (moving towards the left). The means enveloped by the standard deviation of three major forest biomes (tropical, temperate and tropical) are highlighted below.

when the fractions of the BGP effects compared to BGC effects lie between  $-57.2$  and  $24.4\%$  (median  $-10.6\%$ ) at temperate sites and  $-32.6$ – $23.7\%$  (median  $-4.1\%$ ) at boreal ones. Forest areas that exert a BGP warming see the cooling benefit of the BGC effect reduced by  $-63.7$  to  $-1.8\%$  (median  $-18.5\%$ ) in temperate and  $-36.7$  to  $-0.7\%$  (median  $-10.3\%$ ) in boreal regions during winter. The more pronounced adverse winter warming of temperate sites diverges from previous studies, which find boreal forests more heavily affected<sup>8,9</sup>. In our assessment, temperate sites experience stronger warming effects than boreal sites in winter only in relation to their carbon uptake and only if the soil carbon storage is assessed alongside the above-ground biomass. Boreal sites are associated with more soil carbon uptake or removal than temperate sites, which diminishes the fraction of BGP-induced warming compared to the BGC effect. The warming signal of the BGP effects used in this study is in line with preceding work in locating the strongest winter warming signal in boreal zones.

Neglecting this seasonality might lead to efforts that underestimate the cooling benefits to adaptation during the summer when heat stress might be the most taxing to humans and the environment but also runs the risk of not considering the adverse impacts of winter warming. Many pests and invasive species that attack trees and diminish biodiversity are held back in their spread due to winter temperatures that are too low for them to tolerate. An increase in local winter temperature due to BGP effects can add to the pressure that ecosystems are already exposed to due to climate change<sup>25–27</sup>.

Tropical forestation and forest conservation do not induce a local warming influence in any season. Further, they demand  $3.6$ – $3.7\times$  less area to achieve the same  $\text{CO}_2\text{e}$  of BGP and BGC effects compared to temperate and boreal forests. A smaller land demand is highly important since forests compete with other land-use demands such as BECCS or food production.

We find far fewer non-forested sites (current grassland, cropland or shrubland) where establishing a neighbouring (within a  $0.25^\circ \times 0.25^\circ$  window) forest exerts a cooling influence of similar magnitude to the cooling effect of conserving standing forest sites. More than a third ( $36.6\%$ ,  $1,058 \text{ Mha}$ ) of all current forest cover holds an equal or higher mitigation potential if conserved than the 95th percentile ( $601.4 \text{ tCO}_2\text{e ha}^{-1}$ ,  $117 \text{ Mha}$ ) effect of establishing a

forest on a currently non-forested site (Fig. 4). Large-scale reforestation efforts such as the Bonn Challenge, which aims to establish  $350 \text{ Mha}$  of forests on currently degraded and deforested land by 2030 (<https://www.bonnchallenge.org/>), will also need to consider less effective sites due to the limited non-forested area on which forestation could achieve a mitigation potential comparable to the conservation of standing tropical forests (Fig. 4).

The high BGP and BGC impact of tropical forests on climate suggests that future intensification of land use in these areas will have a more substantial adverse effect than historical deforestation of temperate forests (tropical mean of standing forests  $790.2 \text{ tCO}_2\text{e ha}^{-1}$  ( $\sigma = 105.6 \text{ tCO}_2\text{e ha}^{-1}$ ) versus temperate forestation sites  $167.0 \text{ tCO}_2\text{e ha}^{-1}$  ( $\sigma = 104.1 \text{ tCO}_2\text{e ha}^{-1}$ )). In addition, tropical rainforests are further at risk from climate change itself, which is estimated to have an impact similar in size to anthropogenic deforestation<sup>28–30</sup>. Our assessment of both the BGC and local BGP effect reinforces findings that established the high importance of conserving tropical forests for climate change mitigation<sup>13</sup>.

Combining the observationally constrained BGC and local BGP effect highlights the big regional differences in the suitability of forestation and forest conservation sites of previous model-based studies<sup>8–10,13</sup>. Tropical rainforests exceed all other forests in terms of their combined BGC and local BGP mitigation potential. These highly beneficial sites are predominantly still forested and might be conserved while the area available to reforestation or afforestation with a comparable mitigation potential is limited. Further, we show that the focus on annual BGP effects masks their pronounced seasonality at higher latitudes.

The observation-based data on the BGP effect used here differ in their limitations from modelled data used in previous studies. We discuss these caveats and their implications in the following. (1) First, the observational datasets only depict the local effect on temperature. While these local impacts are of immediate relevance to ecosystem behaviour and human health, model experiments suggest that the non-local effects might be more critical to global climate, especially for the change in surface albedo<sup>31</sup>. Thus, our implementation of the warming effect of a lowered albedo is probably too conservative in assuming only a local impact. Further, we do not consider teleconnections produced by large-scale forestation

potentially changing atmospheric circulation like a shift of the inter-tropical convergence zone<sup>22</sup>. (2) Remote sensing data are limited to non-overcast conditions, overestimating the effect of the local albedo and evaporative changes experienced under cloud cover. The dataset produced by Duvellier et al.<sup>17</sup> solely relies on remote sensing data, while Bright et al.<sup>16</sup> also includes station data that do not suffer from this caveat. (3) Satellites report the temperature at the surface instead of 2 m above it. The latter, more commonly discussed metric, could be influenced differently by BGP effects. (4) The reported BGP impacts are valid under current climate. The change of environmental variables due to climate change like the duration and extent of snow cover cannot be considered with remote sensing data. Thus, we probably overestimate the winter warming of high latitude forests, which is strongly tied to the snow cover, especially in high-emission scenarios where temperatures are much higher than today. Further, the location and extent of forested ecozones discussed in our study would probably change in a world many degrees warmer than today. The more we are able to curb the warming trajectory the less pronounced this issue will be. Thus, our estimates of the BGP effect are most valid and best applied in low-emission scenarios.

We use the local, rather than global, mean TCRE response to translate the BGP effect to its CO<sub>2</sub>e. This implies that the same local BGP-induced temperature change at two different locations does not necessarily yield the same BGP CO<sub>2</sub>e since the emitted carbon responsible for the same temperature change can differ between given locations. The local BGP effect is, thus, weighted by the sensitivity of the local climate to CO<sub>2</sub> emissions. In a region experiencing a strong climate response to CO<sub>2</sub> emissions, the BGP-induced temperature change is equivalent to fewer carbon emissions. At continental high latitudes, the temperature response to CO<sub>2</sub> emissions can be almost twice as high compared to coastal, low latitudes (Supplementary Fig. 1). Therefore, the same BGP-induced temperature change would be equivalent to almost twice the CO<sub>2</sub>e in the last regions. This implicit weighting is intended since the BGP temperature change will achieve a smaller share in comparison to the local climate change signal of the BGC effect if the local sensitivity to CO<sub>2</sub> is high. A display of Figs. 1 and 3 produced by the global mean instead of the local TCRE translation of the BGP effect is given in Extended Data Figs. 1 and 2.

Our observationally constrained assessment shows that BGP effects are important to the overall climate benefit of forests, either enhancing or counteracting their mitigation potential (BGC effect). Mitigation policy and scenarios will be more effective if they include BGP processes and their implementation is necessary to avoid potential counterproductive actions. We provide a map of the influence of both BGP and BGC effects of forests on climate to advance efforts to include BGP effects in land-based mitigation efforts and integrated assessment modelling.

### Online content

Any methods, additional references, Nature Research reporting summaries, source data, extended data, supplementary information, acknowledgements, peer review information; details of author contributions and competing interests; and statements of data and code availability are available at <https://doi.org/10.1038/s41558-021-01161-z>.

Received: 14 October 2019; Accepted: 24 August 2021;  
Published online: 27 September 2021

### References

- IPCC *Special Report on Global Warming of 1.5 °C* (eds Masson-Delmotte, V. et al.) (WMO, 2018).
- IPCC *Special Report on Climate Change and Land* (IPCC, 2019).
- Intended Nationally Determined Contributions (INDCs)* <https://www4.unfccc.int/sites/submissions/indc/Submission%20Pages/submissions.aspx> (UNFCCC, 2015); <https://unfccc.int/process-and-meetings/the-paris-agreement/nationally-determined-contributions-ndcs/indcs>
- Erb, K.-H. et al. Unexpectedly large impact of forest management and grazing on global vegetation biomass. *Nature* **553**, 73–76 (2017).
- Griscom, B. W. et al. Natural climate solutions. *Proc. Natl Acad. Sci. USA* **114**, 11645–11650 (2017).
- Ellison, D. et al. Trees, forests and water: cool insights for a hot world. *Glob. Environ. Change* **43**, 51–61 (2017).
- Bonan, G. B. Forests and climate change: forcings, feedbacks, and the climate benefits of forests. *Science* <https://doi.org/10.1126/science.1155121> (2008).
- Betts, R. A. Offset of the potential carbon sink from boreal forestation by decreases in surface albedo. *Nature* **408**, 187–190 (2000).
- Betts, R. A., Falloon, P. D., Goldewijk, K. K. & Ramankutty, N. Biogeophysical effects of land use on climate: model simulations of radiative forcing and large-scale temperature change. *Agric. For. Meteorol.* <https://doi.org/10.1016/j.agrformet.2006.08.021> (2007).
- Bala, G. et al. Combined climate and carbon-cycle effects of large-scale deforestation. *Proc. Natl Acad. Sci. USA* **104**, 6550–6555 (2007).
- Davin, E. L. & de Noblet-Ducoudre, N. Climatic impact of global-scale deforestation: radiative versus nonradiative processes. *J. Clim.* **23**, 97–112 (2010).
- Perugini, L. et al. Biophysical effects on temperature and precipitation due to land cover change. *Environ. Res. Lett.* **12**, 053002 (2017).
- Anderson-Teixeira, K. J. et al. Climate-regulation services of natural and agricultural ecoregions of the Americas. *Nat. Clim. Change* **2**, 177–181 (2012).
- Sonntag, S., Pongratz, J., Reick, C. H. & Schmidt, H. Reforestation in a high-CO<sub>2</sub> world—higher mitigation potential than expected, lower adaptation potential than hoped for. *Geophys. Res. Lett.* **43**, 6546–6553 (2016).
- Gao, F. et al. Multiscale climatological albedo look-up maps derived from moderate resolution imaging spectroradiometer BRDF/albedo products. *J. Appl. Remote Sens.* **8**, 083532 (2014).
- Bright, R. M. et al. Local temperature response to land cover and management change driven by non-radiative processes. *Nat. Clim. Change* <https://doi.org/10.1038/nclimate3250> (2017).
- Duvellier, G., Hooker, J. & Cescatti, A. The mark of vegetation change on Earth's surface energy balance. *Nat. Commun.* **9**, 679 (2018).
- Davin, E. L., de Noblet-Ducoudré, N. & Friedlingstein, P. Impact of land cover change on surface climate: relevance of the radiative forcing concept. *Geophys. Res. Lett.* <https://doi.org/10.1029/2007GL029678> (2007).
- Taylor, K. E., Stouffer, R. J. & Meehl, G. A. An overview of CMIP5 and the experiment design. *Bull. Am. Meteorol. Soc.* **93**, 485–498 (2012).
- Aaron, R. & Gibbs, H. K. *New IPCC Tier-1 Global Biomass Carbon Map for the Year 2000* (Carbon Dioxide Information Analysis Center, 2008); [https://cdiac.ess-dive.lbl.gov/epubs/ndp/global\\_carbon/carbon\\_documentation.html](https://cdiac.ess-dive.lbl.gov/epubs/ndp/global_carbon/carbon_documentation.html)
- Sanderman, J., Hengl, T. & Fiske, G. J. Soil carbon debt of 12,000 years of human land use. *Proc. Natl Acad. Sci. USA* **114**, 9575–9580 (2017).
- Devaraju, N., Bala, G. & Modak, A. Effects of large-scale deforestation on precipitation in the monsoon regions: remote versus local effects. *Proc. Natl Acad. Sci. USA* **112**, 3257–3262 (2015).
- Meier, R. et al. Empirical estimate of forestation-induced precipitation changes in Europe. *Nat. Geosci.* **14**, 473–478 (2021).
- Kirschbaum, M. U. F., Sagar, S., Tate, K. R., Thakur, K. P. & Giltrap, D. L. Quantifying the climate-change consequences of shifting land use between forest and agriculture. *Sci. Total Environ.* <https://doi.org/10.1016/j.scitotenv.2013.01.026> (2013).
- Williams, D. W. & Liebhold, A. M. Climate change and the outbreak ranges of two North American bark beetles. *Agric. Entomol.* **4**, 87–99 (2002).
- Kurz, W. A. et al. Mountain pine beetle and forest carbon feedback to climate change. *Nature* **452**, 987–990 (2008).
- Battisti, A. et al. Expansion of geographic range in the pine processionary moth caused by increased winter temperatures. *Ecol. Appl.* **15**, 2084–2096 (2005).
- Bastin, J.-F. et al. The global tree restoration potential. *Science* **365**, 76–79 (2019).
- Gomes, V. H. F., Vieira, I. C. G., Salomão, R. P. & ter Steege, H. Amazonian tree species threatened by deforestation and climate change. *Nat. Clim. Change* **9**, 547–553 (2019).
- Senior, R. A., Hill, J. K. & Edwards, D. P. Global loss of climate connectivity in tropical forests. *Nat. Clim. Change* **9**, 623–626 (2019).
- Winckler, J., Lejeune, Q., Reick, C. H. & Pongratz, J. Nonlocal effects dominate the global mean surface temperature response to the biogeophysical effects of deforestation. *Geophys. Res. Lett.* **46**, 745–755 (2019).
- Wessel, P. & Smith, W. H. F. A Global, Self-consistent, Hierarchical, High-resolution Shoreline database. *J. Geophys. Res. Solid Earth* **101**, 8741–8743 (1996).
- Wessel, P. et al. The Generic Mapping Tools version 6. *Geochem. Geophys. Geosyst.* **20**, 5556–5564 (2019).

**Publisher's note** Springer Nature remains neutral with regard to jurisdictional claims in published maps and institutional affiliations.

© The Author(s), under exclusive licence to Springer Nature Limited 2021

## Methods

We evaluated the combined BGC and local BGP effect of forestation (reforestation and afforestation) and avoided deforestation. Current grassland, shrubland and cropland of the GLC2000 land-cover map are replaced by a neighbouring forest (within a  $0.25^\circ \times 0.25^\circ$  window) following the constraint used in Duveiller et al.<sup>17</sup>. Forested sites are assumed to be protected from a transition to 'cultivated and managed land'. A cross-reference table links the plant functional types used in the BGP datasets to the land-cover types of the GLC2000 land-cover map (Supplementary Table 1). Given these potential land-cover transitions, we quantify the local BGP effect with two observation-based studies<sup>16,17</sup> and the BGC effect with the IPCC Tier-1 vegetation carbon density map<sup>30</sup> as well as a global map of SOC densities combined with their response to land-use change<sup>31</sup>. The BGP effect is translated into a CO<sub>2</sub>e metric for comparison with the BGC effect. Hereafter, we first describe the datasets and our use of them followed by the method to produce the CO<sub>2</sub>e metric concluding with a description of how uncertainties are considered. Further, the approach is displayed in a simplified schematic in Supplementary Fig. 2.

**CO<sub>2</sub> uptake and storage in the forest biomass.** We use the IPCC Tier-1 global biomass carbon density map<sup>30</sup> combined with the GLC2000 land-cover dataset to estimate the CO<sub>2</sub> uptake induced by forestation (or avoided loss due to forest conservation). The map provides estimates of the carbon density of the living above- and below-ground vegetation for each GLC2000 land-cover type. Next to the land-cover type three additional parameters are taken into account: (1) ecofloristic zones by the Food and Agriculture Organization which considers the specific temperature regime and vegetation type, for example, boreal shrubland or tropical humid forest; (2) continental regions; and (3) whether a forest is an undisturbed 'frontier' forest or a managed, disturbed forest. The respective carbon density is assigned to each unique combination of the above-mentioned parameters and is then mapped to a  $1 \times 1 \text{ km}^2$  grid. The potential CO<sub>2</sub> uptake of forestation or avoided loss of forest conservation ( $\text{CO}_2^{\text{BGC}}(i, j)$ ) is established by comparing carbon densities of forested and non-forested (grassland, shrubland and cropland) land. We produce this difference between the initial ( $\text{CO}_2^{\text{density}}_{\text{ini}}$ ) and transitioned ( $\text{CO}_2^{\text{density}}_{\text{trn}}$ ) land cover for non-forest locations (the CO<sub>2</sub> uptake of forestation) and all forested areas (the avoided emissions from potential deforestation) at latitudes and longitudes ( $i, j$ ).

$$\text{CO}_2^{\text{BGC}}(i, j) = \text{CO}_2^{\text{density}}_{\text{ini}}(i, j) - \text{CO}_2^{\text{density}}_{\text{trn}}(i, j)$$

We adapt a moving-window approach<sup>17,34</sup>, in which the type of forest established at non-forested sites is chosen from a neighbouring location (within a  $0.25^\circ \times 0.25^\circ$  window). If different types of forests exist within a window, we choose the forest type leading to the most beneficial (highest positive) combined BGP and BGC effect, calculated as the sum of BGP and BGC effects in CO<sub>2</sub>e. If no forest occurs in a given window no transition is considered which is in line with the approaches used in the BGP datasets. Because of this, the non-forested area is probably underestimated in parts of the United Kingdom, Uruguay and central Argentina where extensive clear-cutting has left large patches of land without a single site that was recognized as forest in the GLC2000 land-cover dataset. In the case of forest conservation, we assume that deforestation would have led to 'cultivated and managed land'. Thus, the avoided release of carbon by forest conservation is the difference between the initial carbon density of the forest and the cultivated and managed land value in the IPCC biomass assessment.

**CO<sub>2</sub> uptake and storage in the soil.** The global map of SOC store before and after human-induced land-use change used in our study is based on a machine learning model that fits globally acquired SOC datasets with historic land-use estimates and climatic, geographic and lithological variables<sup>21</sup>. It has previously been used to assess the global mitigation potential of SOC stocks<sup>5</sup>. The authors provide a global map of SOC densities before human-induced land-use change and further assess the average stock change in % that can be expected from different land-use changes such as forest converted to cropland or grassland. We combine the SOC densities ( $\text{SOCdensity}(i, j)$ ) with the stock change by land-cover change ( $\text{Loss(LCC)}$ ) to assess the expected CO<sub>2</sub> uptake or release of forestation and avoided deforestation ( $\text{CO}_2^{\text{SOC}}(i, j)$ ).

$$\text{CO}_2^{\text{SOC}}(i, j) = \text{SOCdensity}(i, j) \times \text{Loss(LCC)}$$

Hence, the avoided release of CO<sub>2</sub> from the SOC store by protecting forests amounts to the product of the local SOC density and the expected loss of the conversion from forest to cropping. In line with our approach for biomass and BGP effects we assume that forestation has the reversed effect of deforestation. Thus, the uptake of CO<sub>2</sub> in the SOC store by forestation becomes the product of the local SOC density and the expected increase in SOC storage.

SOC stores can take years to decades or even hundreds of years to reach a new equilibrium after land-use change. To stay within the chosen time frame of end-of-century responses we limit the SOC density and stock change to the top 30 cm of soil.

**BGP response to forestation and forest conservation.** Two observation-based studies provide us with the potential local surface temperature response due to transitions between plant functional types on a  $1^\circ$  grid<sup>16,17</sup>. The change in surface energy balance leading to the temperature response is quantified by either only remote sensing<sup>17</sup> or also in situ observations<sup>16</sup>. The global coverage of the two datasets differs due to the methods that were applied. Wherever both studies overlap and yield a data point at the same location we produce a mean, upper- and lower-bound between the two. Potential transitions are restricted to plant functional types that occur in the same Koeppen-Geiger climate zone or to types that are present within a  $0.25^\circ \times 0.25^\circ$  window.

**Metric used to compare BGP and BGC impacts.** Previous studies compared the radiative forcing of the BGP and BGC effect<sup>8,35</sup>. This approach neglects non-radiative processes such as changes in evapotranspiration and surface roughness relevant to the local climate<sup>18</sup>. We refrain from using radiative forcing to also encompass these non-radiative effects and translate the BGP-induced local temperature change ( $\Delta^\circ\text{C}_{\text{BGP}}$ ) into a CO<sub>2</sub>e metric ( $\text{CO}_2^{\text{BGP}}$ ). This metric represents the CO<sub>2</sub> emissions that would theoretically produce the same local temperature response. This requires to first derive the global CO<sub>2</sub> emission that would induce a temperature change of the same magnitude in the grid cell under consideration. To this end, a local transient climate response (TCRE( $i, j$ )) is used which estimates the transient surface temperature response to cumulative CO<sub>2</sub> emission at each grid cell using the +1% pCO<sub>2</sub> increase per year experiments<sup>19</sup> of 21 CMIP5 models (ACCESS1-0; bcc-csm1-1; BNU-ESM; CCSM4; CNRM-CM5; CSIRO-Mk3-6-0; EC-EARTH; FGOALS-s2; GFDL-ESM2G; GISS-E2-H; HadGEM2-ES; ACCESS1-3; bcc-csm1-1-m; CanESM2; CNRM-CM5-2; CSIRO-Mk3L-1-2; FGOALS-g2; GFDL-CM3; GFDL-ESM2M; GISS-E2-R; Inmcm4) (Supplementary Fig. 1). To be consistent with the remote sensing datasets<sup>16,17</sup>, we use the surface temperature response as opposed to the standard 2-m temperature. The transient temperature response is defined as the difference between the experimental runs after a doubling of atmospheric CO<sub>2</sub> and the equilibrium temperature at pre-industrial CO<sub>2</sub> levels at the beginning of the experiment. In line with the proposed protocol in the Fifth Assessment Report (AR5, ref. <sup>36</sup>) we assess mean surface temperatures for the time between 20 yr before and after the doubling of global, atmospheric CO<sub>2</sub> concentrations in the experimental runs. We then assume a linear relationship between the increase in global CO<sub>2</sub> concentration and the transient surface temperature response. As a second step, we divide the resulting global CO<sub>2</sub>e by the Earth's surface area ( $A_{\text{SFC}}$ ) to scale the global emission equivalent to the local contribution of the considered grid cell as follows:

$$\text{CO}_2^{\text{BGP}}(i, j) = \frac{\Delta^\circ\text{C}_{\text{BGP}}(i, j)}{\text{TCRE}(i, j)} \times \frac{1}{A_{\text{SFC}}}$$

We compare this CO<sub>2</sub>e<sup>BGP</sup> to the potential CO<sub>2</sub> uptake or avoided emission from reforesting or afforesting and protecting forests ( $\text{CO}_2^{\text{BGC}}$ ).

The climate response experiments on which the TCRE is based are driven by a doubling of airborne CO<sub>2</sub> and not emissions, the latter being buffered by natural sinks. Hence, to use the TCRE to relate local temperature changes to emissions rather than atmospheric CO<sub>2</sub> we need to account for the buffering factor which removes half of the emitted CO<sub>2</sub> (ref. <sup>37</sup>) from the atmosphere. Thus, to produce the carbon emission equivalent we multiply the atmospheric CO<sub>2</sub> concentration of the TCRE experiments by two to produce the emissions that would be necessary for the atmospheric carbon concentration. This TCRE based on emissions instead of its previous atmospheric carbon content is used to translate the BGP effect to its emission equivalent.

As an example, a grid cell experiences a warming of 2.1 °C in response to a doubling of atmospheric carbon from 286 to 572 ppm in the TCRE experiment. This doubling of the airborne CO<sub>2</sub> concentration corresponds to the emission of 4,467.3 GtCO<sub>2</sub>. We arrive at this global emission by doubling the ppm difference ( $2 \times (572 - 286)$ ) to account for the buffering by natural sinks and further multiplying by the factor of 7.81 to convert ppm to GtCO<sub>2</sub> (ref. <sup>38</sup>). The same grid cell might be cooled by 1.3 °C ( $\Delta^\circ\text{C}_{\text{BGP}}$ ) by the BGP effects of forestation. Hence, this sites BGP response to forestation corresponds to 54.3 tCO<sub>2</sub>e ha<sup>-1</sup> after dividing by local TCRE and the Earth's surface area.

**Dealing with uncertainty.** Four different kinds of dataset are used in our study: (1) data on the biomass carbon storage, (2) data on the soil carbon storage, (3) data on the local surface temperature response to land-cover transitions and (4) data on the local climate response to cumulative emissions. We produce a mean, high and low estimate for each of the four kinds of dataset. (1) We produce three estimates of the carbon inventory. The IPCC Tier-1 biomass carbon stock map is designated as the mean value. From this, we add/subtract the standard deviation between multiple different carbon stock estimates<sup>4</sup> to get a higher and lower estimate. (2) The SOC response to land-cover transitions is provided with a mean and standard deviation which we apply to the SOC density for given transitions. (3) The two datasets of the local surface temperature change let us deduce an upper- and lower-bound as well as a mean value. (4) In addition to the ensemble mean, we compute the multimodel standard deviation of the climate response to produce an upper- and lower-bound. Thus, we obtain a mean value accompanied by a high

and a low estimate for each variable. We combine the biomass and SOC estimates to produce one mean and high/low estimate for the BGC effect. The median of all combinations (27) between the mean, high and low datasets of the BGP and BGC response as well as the climate response is depicted in figures and numbers.

### Data availability

The data on the combined BGC and BGP impact of forestation and forest conservation, as well as the BGP impact on its own, are available on Zenodo (<https://doi.org/10.5281/zenodo.5184884>)<sup>39</sup>.

### Code availability

The Geospatial Data Abstraction Library v.2.4.1 and QGIS 2.18 were used with Python 3.6.5 to process and assess the described datasets. The code is available on Zenodo (<https://doi.org/10.5281/zenodo.5211680>)<sup>40</sup> and GitHub (<https://github.com/mikewin-climsci/BGPvBGC.git>).

### References

34. Lejeune, Q., Seneviratne, S. I. & Davin, E. L. Historical land-cover change impacts on climate: comparative assessment of LUCID and CMIP5 multimodel experiments. *J. Clim.* <https://doi.org/10.1175/JCLI-D-16-0213.1> (2017).
35. Schwaab, J. et al. Carbon storage versus albedo change: radiative forcing of forest expansion in temperate mountainous regions of Switzerland. *Biogeosci. Discuss.* **11**, 10123–10165 (2014).
36. Myhre, G. et al. in *Climate Change 2013: The Physical Science Basis* (eds Stocker, T. F. et al.) Ch. 12.5.4 (Cambridge Univ. Press, 2013).
37. Le Quéré, C. et al. Global carbon budget 2018. *Earth Syst. Sci. Data* **10**, 2141–2194 (2018).
38. Clark, W. C. *Carbon Dioxide Review: 1982* 467 (Oxford Univ. Press, 1982); <https://www.osti.gov/biblio/6438207>
39. Windisch, M. G., Davin, E. L. & Seneviratne, S. I. Prioritizing forestation based on biogeochemical and local biogeophysical impacts—data (v1.0.0) [Dataset]. *Zenodo* <https://doi.org/10.5281/zenodo.5184884> (2021).
40. Windisch, M. G. Prioritizing forestation based on biogeochemical and local biogeophysical impacts—code (v1.0.0). *Zenodo* <https://doi.org/10.5281/zenodo.5211680> (2021).

### Acknowledgements

We thank T. Crowther for valuable discussions during the conception of this study and J. Schwaab for technical assistance and guidance. This research received funding from the German Federal Ministry of Education and Research (BMBF) and the German Aerospace Center (DLR) via the LAMACLIMA project as part of AXIS, an ERANET initiated by JPI Climate (<http://www.jpi-climate.eu/AXIS/Activities/LAMACLIMA>), last access: 09 September 2021, grant no. 01LS1905A), with co-funding from the European Union (grant no. 776608).

### Author contributions

E.L.D. and S.I.S. conceived the study, which was then further developed by M.G.W. M.G.W. performed the analysis and wrote the first draft of the manuscript. All authors together interpreted the results and edited the manuscript.

### Competing interests

The authors declare no competing interests.

### Additional information

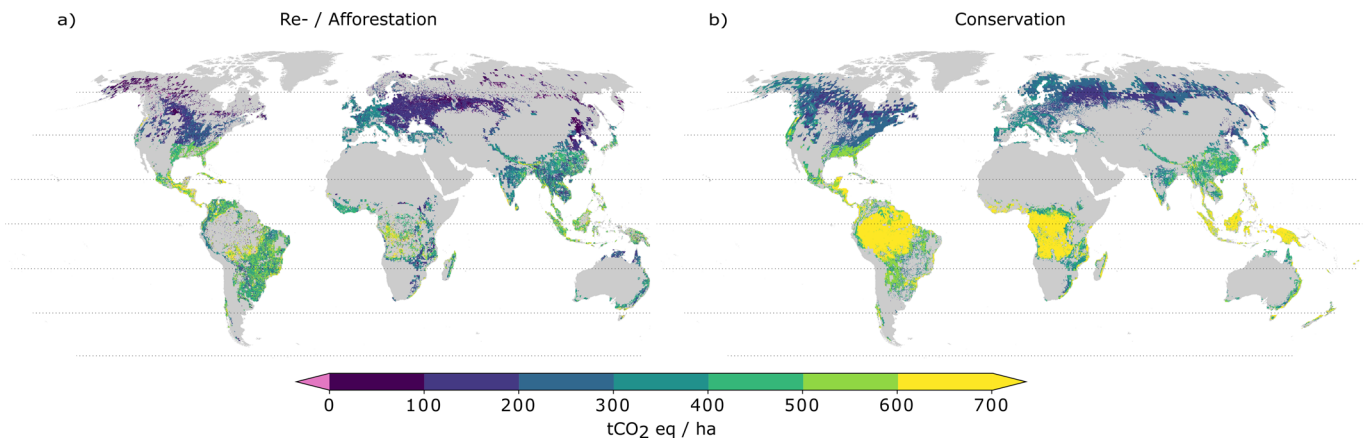
**Extended data** is available for this paper at <https://doi.org/10.1038/s41558-021-01161-z>.

**Supplementary information** The online version contains supplementary material available at <https://doi.org/10.1038/s41558-021-01161-z>.

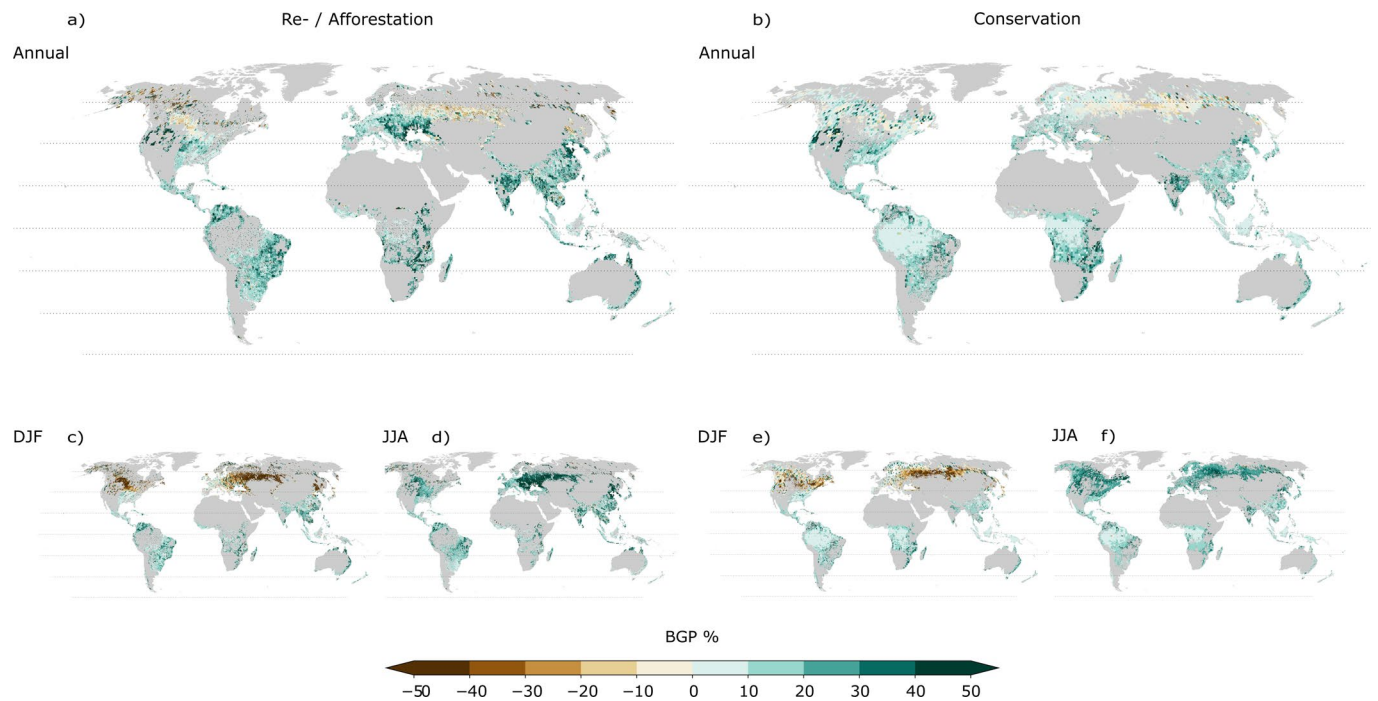
**Correspondence and requests for materials** should be addressed to Michael G. Windisch or Edouard L. Davin.

**Peer review information** *Nature Climate Change* thanks Lucia Perugini and the other, anonymous, reviewer(s) for their contribution to the peer review of this work.

**Reprints and permissions information** is available at [www.nature.com/reprints](http://www.nature.com/reprints).



**Extended Data Fig. 1 | Combined impact of BGP and BGC effects of forestation and forest conservation on annual climate based on a conversion of the BGP effect to a CO<sub>2</sub> equivalent metric using the global instead of the local TCRE.** Climate impact of forestation a) of current grass-, shrub-, and cropland by a neighbouring forest and avoided deforestation of standing forests b) measured by the sum of their CO<sub>2</sub> uptake (or avoided loss) and the CO<sub>2</sub> equivalent of the local BGP effect induced. The CO<sub>2</sub> equivalent of the local BGP warming or cooling response is produced by the global TCRE value in opposition to the local TCRE response used in the main manuscript. Base map adapted from GSHHG<sup>32</sup> and GMT<sup>33</sup>.



**Extended Data Fig. 2 | Seasonality of the BGP impact of forestation and forest conservation based on a conversion of the BGP effect to a CO<sub>2</sub> equivalent metric using the global instead of the local TCRE.** Fraction of the BGP impact of forestation (reforestation and afforestation) (left) and avoided deforestation (right) expressed as CO<sub>2</sub> equivalent compared to the effect of their CO<sub>2</sub> uptake or avoided loss in percent. The CO<sub>2</sub> equivalent of the local BGP warming or cooling response is produced by the global mean TCRE instead of the local TCRE used in the main manuscript. Fractions are reported for the annual average response of forestation (a) and conservation (b), and the boreal winter response to forestation (c) and conservation (e), as well as the boreal summer response to forestation (d) and conservation (f). Brown colours depict areas where BGP effects oppose the BGC impact, turquoise colours are assigned to areas where the cooling effect of the carbon uptake is locally enhanced by BGP processes. Base map adapted from GSHHG<sup>32</sup> and GMT<sup>33</sup>.